Inorg. Chem. **2006**, *45*, 11030–11034

Layered Lanthanide Molybdate Pillared by Chiral [λ-Mo_2O_4EDTA]$^{2-}$

Junjian Luo and Li Xu*

State Key Laboratory of Structural Chemistry, Fujian Institute of Research on the Structure of Matter, Chinese Academy of Sciences, Fuzhou, Fujian 350002, China

Received June 28, 2006

Hydrothermal reactions of $Na_2[Mo_2O_4EDTA]\cdot 5H_2O$ and $LnCl_3\cdot 6H_2O$ produce the chiral layered lanthanide molybdate oxides pillared by the chiral cluster ligand, $[Ln(H_2O)MoO_4]_2[\lambda\text{-}Mo_2O_4EDTA]$ (Ln = Gd, **1**; Eu, **2**; Tb, **3**; Y, **4**). The tetradentate molybdate bridges Ln^{3+} to form a square grid structure, which is pillared by the chiral cluster ligand, $[\lambda\text{-}Mo_2O_4EDTA]^{2-}$, into a 3-D chiral framework structure. Strong VCD (vibrational circular dichroism) signals confirm the chirality of the bulk oxide materials. These bimetallic oxide materials are of highly thermal stability. The magnetic interactions between the Ln^{3+} ions in **1** and **3** are weak antiferromagnetic.

Introduction

Layered metal oxides are one of the most active areas of materials research. The intense interest in these materials is driven by both their interesting structural diversities and applications such as dye-sensitized solar cells, catalysis, sorption, sensors, molecular electronics, and optical materials, among many others.[1−3] Some of these applications, such as dye-sensitized solar cells, deal with hybrid oxide materials where functionalized organometallic complexes with anchoring carboxylate groups, known as sensitizing dyes, bind to nanocrystalline metal oxide films to transform electrons through the bonds between carboxylate and metal ions on the film surface,[4] while optoelectronic and enantioselective applications are related to their chirality.[5,6] Layered metal oxides allowing a variety of organic or organometallic species in the interlamellar region represent an important subclass of hybrid solids in which complementary properties of the two components are expressed in a single material. The layered metal oxides reported thus far include molybdate,[7] vanadate,[8] metal molybdate,[9] and $MReO_4$[10,11] (M = Cu, Ag), and the organic or metal−organic components are usually organoamines or their metal complexes.[7−11] Lanthanide-containing layered oxides are relatively unexplored although they may exhibit useful luminescent, catalytic, and magnetic properties. Chiral layered oxides are rare with the known examples including $Cu(pzc)_2AgReO_4$,[11] $[C_2N_2H_{10}][Co_{4.2}Zn_{1.8}(PO_4)_4(HPO_4)](H_2O)_{10}$,[12] and $[Zn_{1/4}Cd_{1/4}(N(CH_2PO_3H_{2-x})_3(H_2O)_3)]$.[13] The chirality of the former originates from the helical pillars and that of the latter two from the right- and left-handed helices within the inorganic layers that are achiral. Herein, we report on four unprecedented Ln−Mo bimetallic oxides pillared by the chiral EDTA dimolybdenum(V) cluster, $[Ln(H_2O)MoO_4]_2[\lambda\text{-}Mo_2O_4EDTA]$ (Ln = Gd, **1**; Eu, **2**; Tb, **3**; Y, **4**). As shown in Chart 1, $[Mo_2O_4EDTA]^{2-}$ has been reported to exhibit rapid intramolecular racemization in aqueous solution.[14,15] It is selected as a cluster ligand for several reasons, (a) It contains four potential carboxylate oxygen donor atoms and thus is

* To whom correspondence should be addressed. E-mail: xli@fjirsm.ac.cn.

(1) *Pillared Layered Structures: Currents and Applications*; Mitchell, I. V., Ed.; Elsevier Applied Science: New York, 1990.
(2) *Intercalation Chemistry*; Whittingham, M. S., Jacobson, A. J., Eds.; Academic Press: New York, 1982.
(3) *Inorganic Materials*; Bruce, D. W., O'Hare, D., Eds; Wiley: Chichester, U.K., 1996.
(4) Ushiroda, S.; Ruzycki, N.; Lu, Y.; Spitler, M. T.; Pakinson, B. A. *J. Am. Chem. Soc.* **2005**, *127*, 5158−5162.
(5) Seo, J. S.; Whang, D.; Lee, H.; Sun, S. I.; Oh, J.; Jeon, Y. J.; Kim, K. *Nature* **2000**, *404*, 982−986.
(6) Zheng, L. M.; Whitfield, T.; Wang, X. Q.; Jacobson, A. J. *Angew. Chem., Int. Ed.* **2000**, *39*, 4528−4531.
(7) (a) Hagrman, P. J.; Hagrman, D.; Zubieta, *Angew. Chem., Int. Ed.* **1999**, *38*, 2638−2684 and references therein. (b)Zapf, P. J.; Haushalter, R. C.; Zubieta, J. *Chem. Commun.* **1997**, 321−322.
(8) Maggard, P. A.; Boyle, P. D. *Inorg. Chem.* **2003**, *42*, 4250−4252.
(9) (a) Rarig, R. S.; Lam, R.; Zavalij, P. Y.; Ngala, J. K.; LaDuca, R. L.; Greedan, J. E., Jr.; Zubieta, J. *Inorg. Chem.* **2002**, *41*, 2124−2133. (b) Hagrman, D.; Haushalter, R. C.; Zubieta, J. *Chem. Mater.* **1998**, *10*, 361−365.
(10) Maggard, P. A.; Yan, B.; Luo, J. *Angew. Chem., Int. Ed.* **2005**, *44*, 2553−2556.
(11) Yan, B.; Capracotta, M. D.; Maggard, P. A. *Inorg. Chem.* **2005**, *44*, 6509−6511.
(12) Zhao, J.; Ju, J. J.; Chen, X.; Li, X.; Wang, Y.; Wang, R.; Li, M.; Mai, Z. *J. Solid State Chem.* **2002**, *166*, 369−374.
(13) Krishnamohan Shanna, C. V.; Clearfield, A.; Cabeza, A.; Aranda, M. A. G.; Bruque, S. *J. Am. Chem. Soc.* **2001**, *123*, 2885−2886.
(14) Richard, M. W.; Callahan, K. P. *Inorg. Chem.* **1969**, *11*, 2303−2306.
(15) Blackmer, G. L.; Johnson, K. J.; Roberts, R. L. *Inorg. Chem.* **1976**, *15*, 596−601.

10.1021/ic0611793 CCC: $33.50
Published on Web 12/01/2006

Chart 1. Two Enantiomers (δ and λ) of $[Mo_2O_4EDTA]^{2-}$

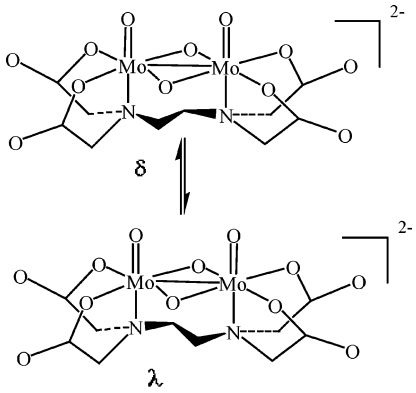

expected to act as a tetradentate ligand in the construction of organic−inorganic hybrid materials. (b) It can be used to prepare chiral materials by resolving two enantiomers through crystallization in a chiral space group. (c) The molybdenum(V) atom may exhibit interesting redox chemistry in self-assembly reactions.

Experimental Section

General Remarks. All chemicals were obtained from commercial sources and used without further purification. IR (KBr pellets) spectra were recorded in the 400−4000 cm^{-1} range using a Perkin-Elmer FT-IR spectrometer. Vibrational circular dichroism (VCD) spectra were measured with the Bruker PMA 37 spectrometer. Elemental analyses were carried out on Elemental Vario EL III microanalyzer. Variable-temperature susceptibility measurements were carried out in the temperature range of 2−300 K at a magnetic field of 0.5 T on polycrystalline samples with a Quantum Design MPMS-5 magnetometer. The thermogravimetric measurements were performed on a Netzsch STA449C apparatus in a nitrogen atmosphere with a heating rate of 10 °C/min from 25 to 800 °C. All syntheses were carried out in 25 mL Teflon-lined autoclaves under autogenous pressure. The reaction vessels were filled to approximately 60% of the volume capacity.

$Na_2[Mo_2O_4EDTA]_2\cdot 5H_2O$. This starting material was synthesized by a modified literature method.[16] HCl (2 M) was added slowly to a stirring aqueous solution (300 mL) of $Na_2MoO_4\cdot 2H_2O$ (15 g, 62.0 mmol), $Na_2S_2O_4$ (5 g, 28.7 mmol), and Na_2H_2EDTA (10.4 g, 31.0 mmol) to adjust the pH to approximately 5, yielding a red solution. The solution was filtered and evaporated in air for several days to produce orange-red crystals of **1** in about a 60% yield.

$[Gd(H_2O)MoO_4]_2[\lambda\text{-}Mo_2O_4EDTA]$ (1). An aqueous solution of $Na_2[Mo_2O_4EDTA]\cdot 5H_2O$ (0.30 g, 0.44 mmol) and $GdCl_3\cdot 6H_2O$ (0.256 g, 0.69 mmol) was heated at 165 °C for 1 day to produce the orange-red crystalline solid of **1** (0.12 g, 35% based on $Na_2[Mo_2O_4EDTA]\cdot 5H_2O$). Anal. Calcd for $C_{10}H_{16}N_2O_{22}Mo_4Gd_2$ (1216.2): C, 9.89; H, 1.33; N, 2.31%. Found: C, 9.86; H, 1.45; N, 2.53%. IR (KBr, cm^{-1}): 1622 (ν_{as}COO), 1398 (ν_sCOO), 959 (Mo═O_t), 758 (ν_{as}, Mo−O_b−Mo), 483(ν_s, Mo−O_b−Mo).

$[Eu(H_2O)MoO_4]_2[\lambda\text{-}Mo_2O_4EDTA]$ (2). The europium oxide **2** was obtained similarly using $EuCl_3\cdot 6H_2O$ instead of $GdCl_3\cdot 6H_2O$. Anal. Calcd for $C_{10}H_{16}N_2O_{22}Mo_4Eu_2$ (1210.9): C, 9.98; H, 1.34; N, 2.33%. Found: C, 10.07; H, 1.43; N, 2.50%. IR (KBr, cm^{-1}): 1619 (ν_{as}COO), 1401 (ν_sCOO), 959 (Mo═O_t), 758 (ν_{as}, Mo−O_b−Mo), 483 (ν_s, Mo−O_b−Mo).

$[Tb(H_2O)MoO_4]_2[\lambda\text{-}Mo_2O_4EDTA]$ (3). The terbium oxide **3** was prepared similarly using $TbCl_3\cdot 6H_2O$ instead of $GdCl_3\cdot 6H_2O$. Anal. Calcd for $C_{10}H_{16}N_2O_{22}Mo_4Tb_2$(1217.8): C, 9.85; H, 1.31; N, 2.30; Mo, 31.51; Tb, 26.10%. Found: C, 9.95; H, 1.55; N, 2.32; Mo, 32.05; Tb, 26.37. IR (KBr, cm^{-1}): 1619 (ν_{as}, COO), 1401 (ν_s,COO), 959 (Mo═O_t), 761 (ν_{as}, Mo−O_b−Mo), 484 (ν_a, Mo−O_b−Mo).

$[Y(H_2O)MoO_4]_2[\lambda\text{-}Mo_2O_4EDTA]$ (4). The yttrium oxide 4 was prepared similarly using $YCl_3\cdot 6H_2O$ instead of $GdCl_3\cdot 6H_2O$. Anal. Calcd for $C_{10}H_{16}N_2O_{22}Mo_4Y_2$ (1077.83): C, 11.14; H, 1.50; N, 2.60%. Found: C, 11.16; H, 1.80; N, 2.67. IR (KBr, cm^{-1}): 1623 (ν_{as}COO), 1401 (ν_sCOO), 962 (Mo═O_t), 763 (ν_{as}, Mo−O_b−Mo), 488 (ν_a, Mo−O_b−Mo).

X-ray Crystallographic Study. Suitable single crystals of **1** and **2** were mounted on a Siemens Smart CCD diffractometer equipped with graphite-monochromated Mo Kα radiation (λ = 0.71073 Å) at 293 K. Absorption corrections were performed using the SADABS program. Structures were solved by direct methods and refined by full-matrix least-squares fitting on F^2 by SHELXTL-97.[17] Non-hydrogen atoms were refined with anisotropic thermal parameters. Hydrogen atoms were located at geometrically calculated positions and treated by a mixture of independent and constrained refinement. Crystallographic data and structural refinements for compounds **1** and **2** are summarized in Table 1. Selected bond lengths are summarized in Table 2. Compounds **3** and **4** are isomorphous with **1** and **2**.

Table 1. Crystallographic Data for **1** and **2**

	1	**2**
formula	$C_{10}H_{16}N_2O_{22}GdMo_4$	$C_{10}H_{16}N_2O_{22}EuMo_4$
fw	1214.51	1203.93
cryst syst	monoclinic	monoclinic
space group	C_2	C_2
a (Å)	10.2998(6)	10.3383(18)
b (Å)	10.5426(6)	10.5558(12)
c (Å)	12.0585(7)	12.0421(4))
β (deg)	109.832(5)	12.0715(18)
vol (Å^3)	1231.73(12)	1239.3(3)
Z	2	2
d_{calcd} (g cm^{-3})	3.275	3.226
μ (mm^{-1})	7.385	7.049
GOF	1.554	0.914
R1 [$I > 2\sigma(I)$]	0.0346	0.0208
ωR2 [$I > 2\sigma(I)$]	0.0906	0.0394
R1 (all data)	0.0362	0.0215
ωR2 (all data)	0.0917	0.0396
Flack param	−0.064(15)	−0.021(10)

Results and Discussion

Synthesis. The dimolybdenum(V) EDTA dianion, $[Mo_2O_4EDA]^{2-}$ was previously prepared by combining Mo(V) solution (prepared by reduction of a Mo(VI) solution with mercury in the presence of hydrochloric acid) and H_4EDTA and by adding potassium hydroxide to adjust the pH.[16] In the present work, a new synthetic method was developed by using the redox reaction of Na_2MoO_4 and $Na_2S_2O_4$ (instead of mercury) in the presence of Na_2H_2EDTA. The pH was adjusted to approximately 5 using 2 M HCl. The reaction runs quickly and smoothly to give $Na_2[Mo_2O_4EDTA]$ in moderate yield, thus providing a

(16) Pecsok, R. L.; Sawyer, D. T. *J. Am. Chem. Soc.* **1956**, *78*, 5496−5500.

(17) Sheldrick, G. M. *SHELXS 97, Program for Crystal Structure Solution*; University of Göttingen: Göttingen, Germany, 1997.

Table 2. Selected Bond Lengths (Å) for **1** and **2**[a]

				1			
Gd−O(1)	2.294(10)	Gd−O(8)	2.372(8)	Mo(2)−O(4)	1.767(9)	Mo(3)−O(7)	2.096(10)
Gd−O(2)#1	2.326(9)	Gd−O(11)	2.442(8)	Mo(3)−O(9)	1.701(9)	Mo(3)−N(1)	2.437(11)
Gd−O(4)#2	2.330(9)	Mo(1)−O(2)	1.739(9)	Mo(3)−O(10)	1.930(8)	Mo(3)−Mo(3)#4	2.564(2)
Gd−O(3)	2.337(9)	Mo(1)−O(1)	1.770(10)	Mo(3)−O(10)#4	1.931(8)		
Gd−O(6)	2.357(7)	Mo(2)−O(3)	1.751(9)	Mo(3)−O(5)	2.077(9)		
				2			
Eu−O(2)#1	2.303(5)	Eu−O(6)	2.379(4)	Mo(2)−O(3)	1.767(5)	Mo(3)−O(5)	2.091(5)
Eu−O(1)	2.309(5)	Eu−O(11)	2.427(5)	Mo(3)−O(9)	1.695(5)	Mo(3)−N(1)	2.425(5)
Eu−O(3)	2.320(5)	Mo(1)−O(1)	1.761(5)	Mo(3)−O(10)	1.938(4)	Mo(3)−Mo(3)#4	2.561(1)
Eu−O(4)#2	2.341(5)	Mo(1)−O(2)	1.763(5)	Mo(3)−O(10)#4	1.952(4)		
Eu−O(8)	2.371(4)	Mo(2)−O(4)	1.750(5)	Mo(3)−O(7)	2.077(5)		

[a] Symmetry code: #1 $-x+1/2, y+1/2, -z+1$; #2 $-x+1/2, y-1/2, -z+1$; #3 $-x, y, -z+1$; #4 $-x, y, -z$.

convenient and economic route to this dimolybdenum(V) EDTA complex. The reactions of $Na_2[Mo_2O_4EDTA]$ and $LnCl_3$ (Ln = Tb, Y, Gd, Eu) are initially designed to prepare cluster-based polymeric materials via extended Ln-O(EDTA) bonds. Interestingly, the oxidization of $Na_2[Mo_2O_4EDTA]$ to tetraoxomolybdate occurs under hydrothermal conditions. The mechanism of formation of **1**−**4** is not clear, but some speculation may be made at this stage. The final products are the bimetallic oxide $[Ln(H_2O)MoO_4]_2[\lambda\text{-}Mo_2O_4EDTA]$ rather than the lanthanide molybdate $Ln_2(MoO_4)_3$, indicating that MoO_4^{2-} is trapped by the $[Mo_2O_4EDTA]$-coordinated Ln^{3+} ($Ln-[Mo_2O_4EDTA]^{2-}$) rather than by a single Ln^{3+} ion. Interestingly, only $[\lambda\text{-}Mo_2O_4EDTA]^{2-}$ in the chiral oxide materials **1**−**4** is formed from several reactions (above six times) under similar hydrothermal conditions. The use of different lanthanide ions such as Gd^{3+}, Eu^{3+}, Y^{3+} and Tb^{3+} gives the same results. The λ and δ forms are convertible to each other through symmetry elements such as invention center, mirror, or glid mirror, but the absence of these symmetry elements in a chiral space group will result in single configuration present in the solid state, exclusively. This offers the opportunity to obtain the chiral solid-state materials based on $[Mo_2O_4EDTA]^{2-}$ through crystallization processes that may yield crystals of chiral space groups as exemplified in the present case. It should be noted that hydrothermal syntheses of molybdate-based heterometallic hybrid oxide materials is a very active area of research and a number of novel materials incorporating transition metal ions have been reported.[7a,9] It is surprising that no related lanthanide−molybdate-based materials is a documented in the literature although lanthanide molybdates have received extensive attention because of their coupled ferroelectic and ferroelectric properties.[18] This may be the result of the much weaker basicity of lanthanide (III) ions than the above-mentioned transition metal ions, which makes the bonding between Ln^{3+} and organoamines employed in the literature much weaker and thus unstable under hydrothermal conditions.[7−11] The use of highly acidic ligands such as carboxylate ligands in the present work obviously favors the formation of stable Ln^{3+}-containing oxide materials. Moreover, the sources of molybdenum are usually molybdnum(VI) oxides such as MoO_3 or MoO_4^{2-}. In the present case, the low-valent molybdenum(V), which is coordinated to the multifunctional ligand (EDTA), serves as a source of the molybdate subunit, presumably providing a new synthetic methodology for the development of the molybdate-based hybrid materials.

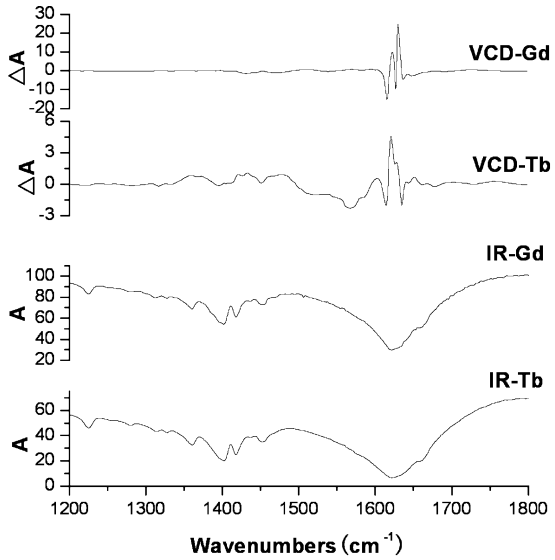

Figure 1. VCD and IR spectra of **1** and **3**.

Crystal Structures. The Gd−Mo bimetallic oxide **1** crystallizes in the chiral space group C_2 and thus only the λ form of $[Mo_2O_4EDTA]^{2-}$ is present in **1**. To determine if all crystals appear as the single λ form rather than a racemic mixture of the λ and δ forms, VCD spectra, a relative new and powerful technique to obtain conformational information of chiral molecules,[19,20] were performed for **1** and **3** as shown in Figure 1. The strong signals appearing in the VCD spectra attributable to the asymmetric C═O strech vibrations confirm the chirality of the bulk crystalline materials.

$[Gd(H_2O)MoO_4]_2[\lambda\text{-}Mo_2O_4EDTA]$ (**1**) consists of the bimetallic oxide layer of $[Cd(H_2O)MoO_4]^+$ that is charge balanced by the chiral dianionic cluster ligand $[\lambda\text{-}Mo_2O_4EDTA]^{2-}$. As in the case of the ferroelectronic−ferroelastic $\beta\text{-}Gd_2(Mo_3O_4)_3$,[20] each Gd^{3+} of **1** has the $[GdO_7]$-mono-capped octahedral coordination geometry with the four equatorial positions being taken up by MoO_4^{2-}, two apical ones by $[\lambda\text{-}Mo_2O_4EDTA]^{2-}$, and the capping one by a

(18) Keve, E. T.; Abrahams, S. C.; Bernstein, J. L. *J. Chem. Phys.* **1971**, *54*, 3185−3194.

(19) Izumi, H.; Yamagami, S.; Futamura, S.; Natie, L. A.; Dukor, R. K. *J. Am. Chem. Soc.* **2004**, *126*, 194−198.

(20) Setnicka, V.; Urbanova, M.; Bour, P.; Kral, V.; Volka, K. *J. Phys. Chem. A.* **2001**, *105*, 8931−8938.

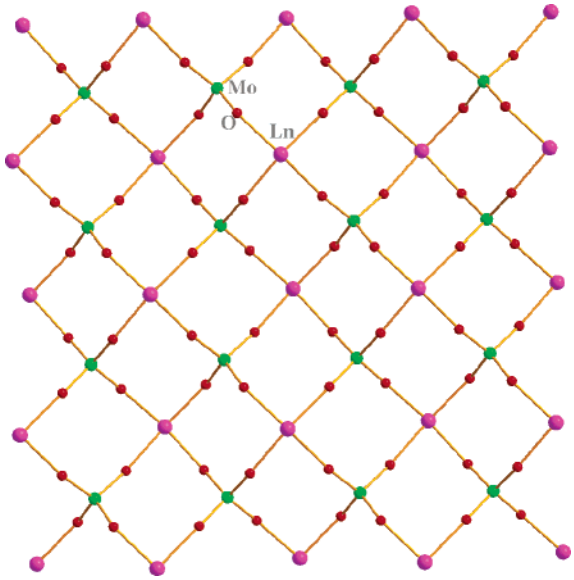

Figure 2. View of the structure of the bimetallic oxide layer.

coordinating water molecule. Each MoO_4^{2-} tetrahedron has a tetradentate ligand that bridges four neighboring Gd^{3+} sites to form an unprecedented undulate square grid structure, as illustrated in Figure 2, differing from the case in [Cu(3,4′-bpy)MoO_4][9] and [Cu(dpe)MoO_4] (dpe = 1,2-trans-(4-pyridyl)ethene),[10] wherein the molybdate is tridentate. This is believed to result from the different coordination requirements of the heterometals. Obviously, the high coordination number of lanthanide ions is responsible for the tetradentate coordinating mode of molybdate in the present case. The 2-D structure of the bimetallic oxide layer features the $Mo_2Gd_2O_4$ eight-membered ring with the deviations of the ring atoms from the least-squares ring plane ranging from 0.07 to 0.39 Å (av 0.238 Å). The Mo−O distances in $[MoO_4]^{2-}$ range from 1.739(9) to 1.767 (9) Å with an average value of 1.757(10) Å, close to those in [Cu(3,4′-bpy)MoO_4][9] (1.730−1.784(2) Å, av 1.758(2) Å) and β-$Gd_2(MoO_4)_3$ (av 1.753(5) Å).[18] The Gd−O bond lengths range from 2.294(10) to 2.357(7) Å with an average value of 2.322(10) Å, slightly shorter than those in β-$Gd_2(Mo_3O_4)_3$ (av 2.332 Å).[18]

The interlamellar region is occupied by the EDTA cluster ligand [λ-Mo_2O_4EDTA]$^{2-}$. The bond lengths and angles in [λ-Mo_2O_4EDTA]$^{2-}$ are not significantly different from those in Na_2[Mo_2O_4EDTA]·$5H_2O$.[21] The [λ-Mo_2O_4EDTA]$^{2-}$ pillar adopts four types of roles in the formation of the hybrid oxide material: (1) a source of molybdate, (2) a source of the chirality, (3) a charge-compensating anion, and (4) a structure-directing ligand to complete the coordination geometry of Gd^{3+}. As illustrated in Figure 3a, the bimetallic oxide layers are linked together by the tetradentate [λ-Mo_2O_4-EDTA]$^{2-}$ pillars through the apical coordinating atoms (O6 and O8) from the terminal oxygen atoms of the cluster ligands to form a 3-D framework structure. The cluster ligands are encapsulated within the channels formed by the ellipsed eight-membered rings as shown in Figure 3b. The Gd−O6 and Gd−O8 distances are 2.357(7) and 2.372(8) Å,

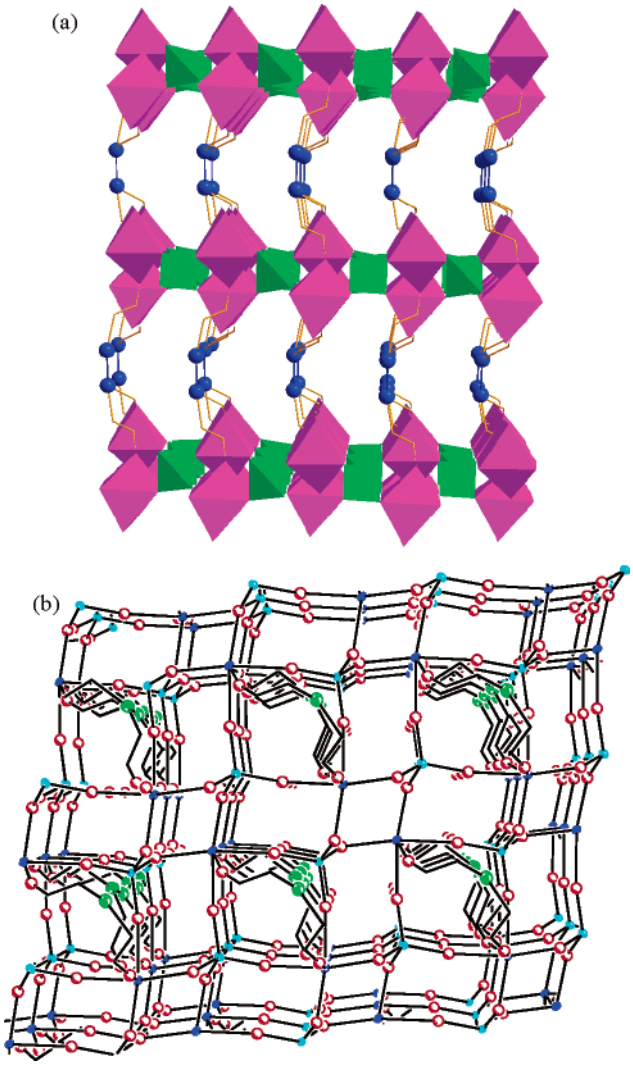

Figure 3. View of the structure of **1** (a) parallel to the metal oxide planes (Mo, green polyhedra; Gd, purple polyhedra), in which some of the atoms of [Mo_2O_4EDTA]$^{2-}$ (Mo, blue) have been omitted for clarity, and (b) perpendicular to the metal oxide planes (Gd, blue; Mo in the oxide layer, cyan; Mo in [Mo_2O_4EDTA]$^{2-}$, green; O, red).

respectively, slightly longer than in the [Gd(H_2O)MoO_4]$^+$ unit but shorter than the Gd−OH_2 distance. The Eu−Mo bimetallic oxide **2** is structurally similar to **1,** and selected bond lengths are listed in Table 2.

Magnetic Properties. The temperature-dependent magnetic susceptibilities of **1**−**3** were recorded over a range of 2−306 K. The plots of μ_{eff} (effective magnetic moment) and $1/\chi_m$ versus T of **1**−**3** are shown in Figure 4. The gadolinium oxide **1** has a μ_{eff} value (7.75 μ_B) similar to the spin-only value (7.94 μ_B) at room temperature. The terbium oxide **3** has a μ_{eff} value (9.42 μ_B) larger than the spin-only value (6.93 μ_B) but similar to the calculated value (9.72 μ_B), based on the spin-orbital coupling at room temperature.[22] The magnetic susceptibility data of **1** and **3** obey the Curie−Weiss law, $\chi_m = C/(T - \theta)$ ($C = 7.69$ cm^3 K mol^{-1}, $\theta = -0.48$ K for **1**; $C = 11.17$ cm^3 K mol^{-1}, $\theta = -5.81$ K for **3**). The small Weiss constants in these complexes reveal the weak antiferromagnetic interactions between the lanthanide ions.

(21) Hong, M. C.; Liu, H. Q. *Chin. J. Struct. Chem.* **1985**, *4*, 34−37.

(22) *Molecular Magnetism*; Kahn, O., Ed.; VCH: New York, 1993.

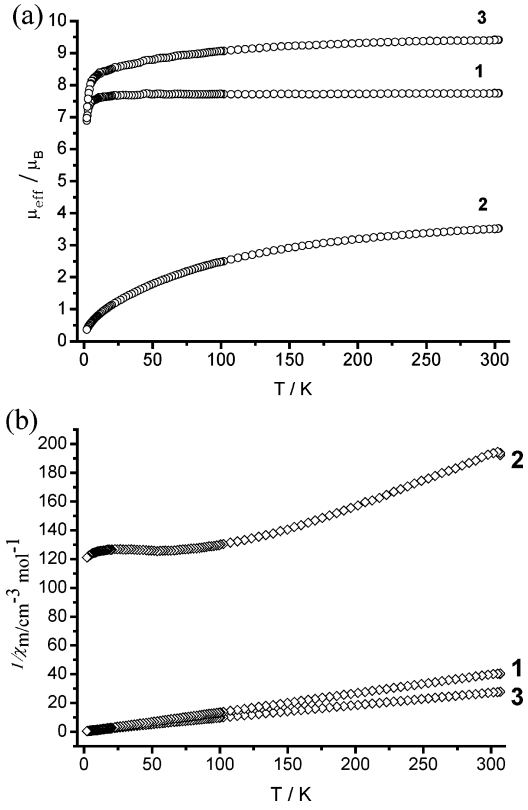

Figure 4. Plots of (a) μ_{eff} and (b) $1/\chi_m$ vs temperature for **1**−**3**.

The europium oxide **2** does not obey the Curie−Weiss because of the small energy gaps and thus the considerable interactions between the ground ($^7F_0$) and lowest excited ($^7F_1$, $^7F_2$, $^7F_3$) states of Eu^{3+}. This leads to the remarkable temperature-dependence of the magnetic susceptibilities and thus the much lower magnetic moments (3.51 μ_B, 300 K; 0.36 μ_B, 1.98 K).

Thermogravimetric Analyses. The TGA curves of **1**−**4** and the starting material $Na_2[Mo_2O_4EDTA]\cdot 5H_2O$ are shown in Figure 5. $Na_2[Mo_2O_4EDTA]\cdot 5H_2O$ clearly loses the lattice water molecules at about 150 °C (12.4%, calcd 13.2%). The complete loss of the coordinating water molecules in **1**−**4** occurs at much higher temperature (**1**, 402; **2**, 378; **3**, 434; **4**, 445 °C). The complete release of the coordinating water molecules is immediately followed by the decomposition of the EDTA ligand, accompanied by the formation of a mixture of Ln_2O_3 (or lanthanide molybdate) and MoO_3, based on their weight percentage (76−78%, calcd 74.4−77.3%) after the second weight loss at about 500 °C. The further weight loss is probably caused by the sublimation of the metal oxides. The loss of EDTA in $Na_2[Mo_2O_4EDTA]\cdot 5H_2O$ presumably produces Na_2MoO_4 and MoO_3 (480 °C, 53.7%, calcd 51.5%), and the further weight loss is accompanied by the decomposition of Na_2MoO_4 to MoO_3 (47.0%, calcd 46.0%).

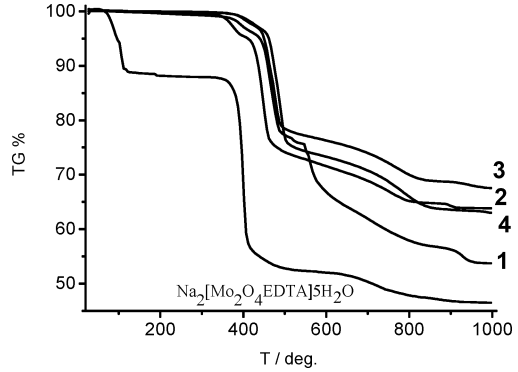

Figure 5. TGA curves of **1**−**4** and $Na_2[Mo_2O_4EDTA]\cdot 5H_2O$.

Conclusion

The unprecedented Ln−Mo bimetallic oxides **1**−**4** have been successfully prepared from the hydrothermal reactions of $LnCl_3$ and the dimolybdenum(V) EDTA cluster ligand. It also reveals the potential of the dianionic EDTA cluster ligand $[Mo_2O_4EDTA]^{2-}$ in the construction of organic−inorganic hybrid materials. These bimetallic oxides crystallize in a chiral space group C_2 and thus appear as chiral materials as confirmed by the VCD spectra.

Acknowledgment. This work was supported by the "One Hundred Talent Program" of Chinese Academy of Sciences.

Supporting Information Available: X-ray crystallographic files in CIF format for **1** and **2**. This material is available free of charge via the Internet at http://pubs.acs.org.

IC0611793